Quantitative Studies of Ground and Excited State Charge Transfer Complexes of Fullerenes with *N,N*-Dimethylaniline and *N,N*-Diethylaniline

Ya-Ping Sun,* Christopher E. Bunker, and Bin Ma

Contribution from the Department of Chemistry, Howard L. Hunter Chemistry Laboratory, Clemson University, Clemson, South Carolina 29634-1905

*Received March 11, 1994**

Abstract: A comprehensive spectroscopic study of ground state charge transfer complexes and exciplexes of C_{60} and C_{70} with *N,N*-diethylaniline (DEA) and *N,N*-dimethylaniline (DMA) is reported. The pure absorption spectra of ground state complexes and pure exciplex fluorescence spectra of C_{60}/C_{70}–DEA/DMA are determined by use of a chemometrics method principal component analysis–self modeling spectral resolution. The exciplex emissions are strongly solvent dependent. In room-temperature toluene, exciplex emissions are absent and the quenching of monomer fluorescence involves both dynamic and static processes. In room-temperature hexane, the quenching of monomer excited state is dominated by the formation of exciplexes. The observed dual fluorescence for C_{60}/C_{70}–DEA/DMA in hexane can be explained by a mechanism in which contributions from both prompt and delayed monomer emissions are considered.

Introduction

The structures and properties of fullerenes C_{60} and C_{70} have attracted a great deal of recent attention.[1] It is known[2] that C_{60} and C_{70} molecules are highly symmetric, representing a special class of aromatic systems. The photochemical and electrochemical properties of the molecules are dominated by the electronic structure of a fully conjugated π-electron shell. Because of the high molecular symmetry, the low-lying electronic transitions of C_{60} are very weak, with a molar absorptivity at the first absorption band maximum of only 940 M^{-1} cm^{-1}.[3] For C_{70}, the transition probabilities are somewhat larger and the maximum molar absorptivity of the first absorption band is 21 000 M^{-1} cm^{-1}.[4] Nevertheless, the fullerenes as fully conjugated π systems have been studied as candidates for novel optical and nonlinear optical materials[5,6] and superconductors.[7] An investigation into C_{60} and C_{70} charge transfer complexes, their formation and properties, should prove beneficial because of the important roles charge transfer materials can play in optical and electronic applications.[8]

It has been reported[9,10] that the absorption and emission spectra of C_{60} and C_{70} in solution undergo significant changes upon the addition of electron donors such as *N,N*-dimethylaniline (DMA) and *N,N*-diethylaniline (DEA). The spectral changes were attributed to the formation of charge transfer complexes. However, a quantitative spectroscopic characterization of the complexes and related photophysical and photochemical properties of the fullerenes has been hindered by the severe spectral overlap of the C_{60} and C_{70} monomer and charge transfer complexes. The fluorescence quantum yields of the fullerenes being very low (2.2×10^{-4} and 5.9×10^{-4} for C_{60} and C_{70} in toluene, respectively)[3,4] also make quantitative experimental measurements somewhat challenging. A clear understanding of the charge transfer properties is very important, especially because the fullerene systems represent interesting examples of charge transfer complexes involving spherical aromatic molecules. In addition, a careful study of the ground and excited state charge transfer reactions will add a new dimension to the understanding of photophysical and photochemical properties of the fullerenes. In this paper, we report a comprehensive spectroscopic investigation of the charge transfer complexes of C_{60} and C_{70} with DEA and DMA. The pure absorption and fluorescence spectra of the complexes are determined by applying a chemometrics spectral resolution method to the observed spectral mixtures. The photophysical properties associated with the formation of the charge transfer complexes are quantitatively evaluated. It is found that emissions from the excited state charge transfer complexes of C_{60}/C_{70}–DEA/DMA are strongly solvent dependent.

Experimental Section

Materials. Buckminsterfullerene-C_{60} from Aldrich (estimated purity >99%), Strem Chemical (purity >99.5%), or MER Co. (purity >99.99%), and (5,6)-fullerene-C_{70} from Strem Chemical (estimated purity >97%) or MER Co. (purity >98%) were used without further purification. Hexane and toluene (both Burdick & Jackson, spectrophotometry grade), *N,N*-dimethylaniline (Aldrich, 99%), and *N,N*-diethylaniline (Aldrich, 99+%) were used as received because no interference from possible impurities in the applied wavelength region was found on the basis of absorption and emission spectroscopic measurements of the materials.

Measurements. Absorption spectra were obtained using a computer-controlled Shimadzu UV-2101PC UV/vis spectrophotometer. While a 10-mm cuvette was used for most measurements, a 2-mm cuvette was employed for the absorption spectra of C_{60} and C_{70} in toluene with DEA and DMA in order to accommodate the wide absorbance variations upon the formation of C_{60}/C_{70}–DEA/DMA ground state complexes.

Fluorescence spectra were recorded on a Spex Fluorolog-2 photon-counting emission spectrometer equipped with a 450-W xenon source and a R928 photomultiplier tube. The fluorescence measurements were made in a right-angle geometry with a 610 nm color glass sharp cut filter (Schott, RG-610) placed before the emission monochromator to eliminate excitation scattering. Spectra thus obtained were corrected for minor

* Abstract published in *Advance ACS Abstracts*, September 15, 1994.

(1) Kroto, H. W.; Allaf, A. W.; Balm, S. P. *Chem. Rev.* **1991**, *91*, 1213.
(2) (a) Fowler, P. W.; Woolrich, J. *Chem. Phys. Lett.* **1986**, *127*, 78. (b) Haddon, R. C.; Brus, L. E.; Raghavachari, K. *Chem. Phys. Lett.* **1986**, *125*, 459.
(3) Sun, Y.-P.; Wang, P.; Hamilton, N. B. *J. Am. Chem. Soc.* **1993**, *115*, 6378.
(4) (a) Sun, Y.-P.; Bunker, C. E. *J. Phys. Chem.* **1993**, *97*, 6770. (b) Catalan, J.; Elguero, J. *J. Am. Chem. Soc.* **1993**, *115*, 9249.
(5) Tutt, L. W.; Kost, A. *Nature (London)* **1992**, *356*, 225.
(6) Meth, J. S.; Vanherzeele, H.; Wang, Y. *Chem. Phys. Lett.* **1992**, *197*, 26 and references cited therein.
(7) Hebard, A. F.; Rosseinsky, M. J.; Haddon, R. C.; Murphy, D. W.; Glarum, S. H.; Palstra, T. T. M.; Ramirez, A. P.; Kortan, A. R. *Nature (London)* **1991**, *350*, 600.
(8) Wang, Y.; Cheng, L.-T. *J. Phys. Chem.* **1992**, *96*, 1530.
(9) (a) Sension, R. J.; Szarka, A. Z.; Smith, G. R.; Hochstrasser, R. M. *Chem. Phys. Lett.* **1991**, *185*, 179. (b) Wang, Y. *J. Phys. Chem.* **1992**, *96*, 764. (c) Caspar, J. V.; Wang, Y. *Chem. Phys. Lett.* **1994**, *218*, 221.
(10) Seshadri, R.; Rao, C. N. R.; Pal, H.; Mukherjee, T.; Mittal, J. P. *Chem. Phys. Lett.* **1993**, *205*, 395.

0002-7863/94/1516-9692$04.50/0 © 1994 American Chemical Society

distortions in the wavelength region close to 610 nm by using the transmittance profile of the filter. However, unless specified otherwise, the reported fluorescence spectra are not corrected for nonlinear instrument response.

The excitation slit was 5 mm (19 nm) for both C_{60} and C_{70} in hexane and toluene. Because the fluorescence spectrum of C_{70} is more structured (especially in hexane), the emission slit for C_{70} was 0.5 mm (1.9 nm). For C_{60}, a larger emission slit (1.25 mm, 4.8 nm) was used in order to increase fluorescence intensities. Under these experimental conditions, the observed fluorescence spectra were weak. In order to reduce random instrumental noise, a relatively long integration time (0.5–1 s per nm) was used. For each experimental condition, 10 to 25 repeat spectra were recorded for better averaging in the data treatment.

The fluorescence lifetimes of C_{60} and C_{70} are short (around 1 ns). It has been reported[3,4] that air-saturation of solutions has essentially no effect on the fluorescence spectra of C_{60} and C_{70}. In the presence of DEA and DMA, the fluorescence spectra of C_{60} and C_{70} in toluene and hexane solutions before and after bubbling with nitrogen gas for ~30 min are the same. Therefore, in our measurements, no special effort was made to deoxygenate all of the solutions.

Data Treatments. A chemometrics method, principal component analysis[11] –self modeling spectral resolution,[12] was used to treat quantitatively the dual emission spectral mixtures.[13-15]

Principal component analysis determines the number of significant components in a linear system.[11] For a data matrix **Y** consisting of n experimental spectra as row vectors, the analysis enables a representation of the spectra in a two-dimensional vector space if each spectrum is a linear combination of two underlying components. The vector space is constructed by two significant eigenvectors of the matrix **Y**, which correspond to two significant eigenvalues. Thus, an experimental spectrum Y_i can be represented as,

$$Y_i = \xi_{i1}V_1 + \xi_{i2}V_2 + R_i \qquad (1)$$

where R_i is a residual vector consisting primarily of experimental noise. If each spectrum in data matrix **Y** is normalized in such a way that the area under the spectrum is unity, the combination coefficients ξ_{i1},ξ_{i2} for experimental spectra adhere to a line (normalization line). For the determination of pure-component spectra, a self modeling spectral resolution method developed by Lawton and Sylvestre was used.[12]

Results

Ground State Complexes. Absorption spectra of C_{60} in toluene and hexane with the presence of an increasing concentration of DEA and DMA were measured at room temperature. In both solvents, observed molar absorptivities of C_{60} increase substantially with increasing DEA and DMA concentration. For example, the observed molar absorptivity at the first band maximum (540 nm) increases from 940 M^{-1} cm^{-1} in neat toluene to 5300 M^{-1} cm^{-1} in neat DMA. The absorption spectral shape also changes with varying DEA and DMA concentration. The first absorption band becomes broader at high DEA and DMA concentrations (Figure 1). The results are in general agreement with those reported earlier for C_{60} in toluene–DMA mixtures.[9a]

The changes in absorption spectra can be attributed to the formation of ground state C_{60}–DEA and C_{60}–DMA complexes.[9a] However, the spectral changes are somewhat similar to those

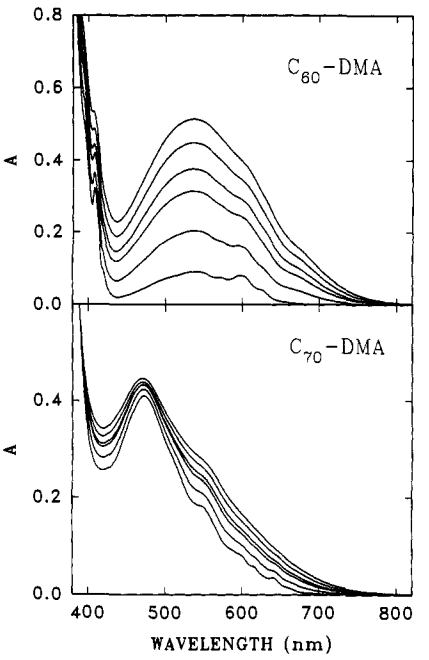

Figure 1. Selected absorption spectra (2-mm optical path) of C_{60} (4.9×10^{-4} M) and C_{70} (9.8×10^{-5} M) as a function of DMA concentration in room temperature toluene. The concentrations of DMA are (for spectra in the order of increasing absorbance) 0, 1.6, 3.4, 4.7, 6.3, and 7.9 (neat DMA) M.

associated with the formation of C_{60} and C_{70} aggregates in room temperature solutions.[16-18] Although the solvent mixtures used here have different characteristics from those in the aggregate formation, the possibility of aggregates was still a concern because of the spectral similarities. A concentration dependent study of C_{60} in neat DMA was performed. With a variation of C_{60} concentration from 5×10^{-6} to 8×10^{-4} M, the absorption spectra are essentially the same, indicating no involvement of C_{60} aggregates.

While the absorption results are consistent with the formation of C_{60}–DEA/DMA ground state complexes, an interesting question is whether the absorption spectra are dominated by C_{60}–DEA/DMA 1:1 complexes or by a distribution of complexes consisting of different numbers of DEA/DMA molecules. The issue was examined by applying principal component analysis to the observed absorption spectral mixtures. For C_{60}–DMA in toluene, the input data matrix for the analysis consisted of 55 rows corresponding to absorption spectra at 11 DMA concentrations from 0 to 7.89 M (neat DMA) with 5 replicates at each DMA concentration. The analysis of the data matrix yielded eigenvalues corresponding to a two-component system. A plot of the combination coefficients ξ_{i1} and ξ_{i2} is linear (Figure 2), also consistent with a two-component system. Because one of the two pure components is the C_{60} monomer, the result suggests that there is only a single absorption spectrum for the C_{60}–DMA complexes. It is likely that the spectrum is due to the C_{60}–DMA 1:1 complex, unless other C_{60}–DMA complexes have the same absorption spectrum.

A similar treatment was performed for the absorption spectra of C_{70}–DMA in toluene. For C_{70}, while the absorption spectra become broader as the DMA concentration increases, observed absorbance at the first band maximum only increases slightly (Figure 1). The input data matrix for principal component analysis consisted of 36 rows corresponding to absorption spectra recorded at 12 different DMA concentrations (3 repeat measurements at each concentration) from 0 to 7.89 M (neat DMA). Both the relative magnitude of the eigenvalues and the plot of

(11) Malinowski, E. R. *Factor Analysis in Chemistry*, 2nd ed.; Wiley: New York, 1991.
(12) Lawton, W. H.; Sylvestre, E. A. *Technometrics* **1971**, *13*, 617.
(13) For reviews see: (a) Ramos, L. S.; Beebe, K. R.; Carey, W. P.; Sanchez, E. M.; Erickson, B. C.; Wilson, B. E.; Wangen, L. E.; Kowalski, B. R. *Anal. Chem.* **1986**, *58*, 294R. (b) McGown, L. B.; Warner, I. M. *Anal. Chem.* **1990**, *62*, 255R.
(14) For an application to *trans*-1-(2-naphthyl)-2-phenylethene–amine exciplexes see: (a) Eaker, D. W. Ph.D. Dissertation, Florida State University, 1984. (b) Choi, J.-O. Ph. D. Dissertation, Florida State University, 1992. (c) Saltiel, J., unpublished results.
(15) For typical applications see: (a) Sylvestre, E. A.; Lawton, W. H.; Maggio, M. S. *Technometrics* **1974**, *16*, 353. (b) Osten, D. W.; Kowalski, B. R. *Anal. Chem.* **1984**, *56*, 991. (c) Aartsma, T. J.; Gouterman, M.; Jochum, C.; Kwiram, A. L.; Pepich, B. V.; Williams, L. D. *J. Am. Chem. Soc.* **1982**, *104*, 6281. (d) Sun, Y.-P.; Sears, D. F., Jr.; Saltiel, J.; Mallory, F. B.; Mallory, C. W.; Buser, C. A. *J. Am. Chem. Soc.* **1988**, *110*, 6974. (e) Tauler, R.; Kowalski, B.; Fleming, S. *Anal. Chem.* **1993**, *65*, 2040. (f) Bunker, C. E.; Hamilton, N. B.; Sun, Y.-P. *Anal. Chem.* **1993**, *65*, 3460.
(16) Sun, Y.-P.; Bunker, C. E. *Nature (London)* **1993**, *365*, 398.
(17) Sun, Y.-P.; Bunker, C. E. *Chem. Mater.* **1994**, *6*, 578.
(18) Sun, Y.-P.; Bunker, C. E.; Ma, B., manuscript in preparation.

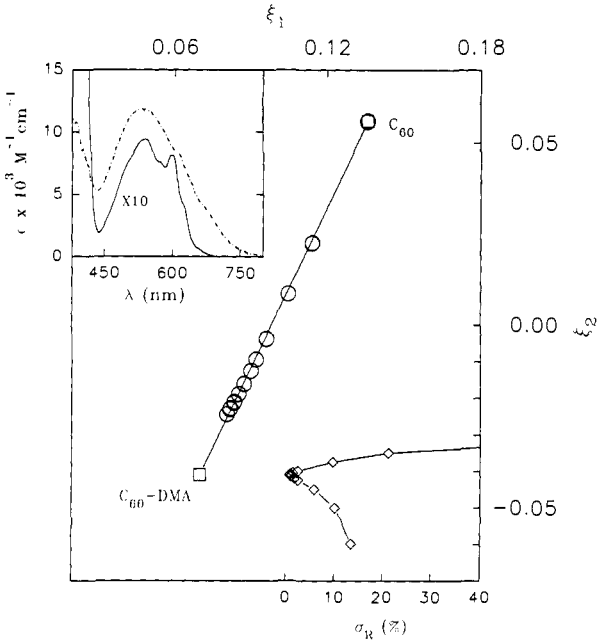

Figure 2. Plots of combination coefficients and relative standard deviations (σ_R) for the determination of the C_{60}–DMA limit. The insert shows the absorption spectra of the C_{60} monomer (—) and the C_{60}–DMA complex (– • –) from the spectral resolution method.

combination coefficients are consistent with a two-component system (Figure 2). Again, it is likely that the charge transfer absorption spectrum is dominated by the C_{70}–DMA 1:1 complex.

The pure absorption spectra of C_{60}–DMA and C_{70}–DMA complexes were determined by a self modeling spectral resolution method.[12] For the C_{60}–DMA system, the absorption spectrum of the C_{60} monomer is known. It has no contributions in the red onset region, satisfying the Lawton–Sylvestre boundary condition.[12] However, the same boundary condition is not applicable to a determination of the complex absorption band because there is not a wavelength in the entire considered region (380–820 nm) where the monomer has a contribution and the complex does not. Another independent boundary condition is required for a determination of the absorption spectrum of the C_{60}–DMA complex.

A chemical constraint was developed from the conclusion discussed above that the mixtures consist of only the C_{60} monomer and the C_{60}–DMA 1:1 complex. For an observed absorption spectrum i, the absorbance A at a given wavelength is the sum of contributions from the monomer ($A_{M,i}$) and complex ($A_{C,i}$). Because the pure component spectra from the spectral resolution method are normalized, the corresponding normalized absorbancies at the given wavelength are A_M^0 and A_C^0. There is the following relationship,

$$(x_{C,i}/x_{M,i})(A_C^0/A_M^0) = A_{C,i}/A_{M,i} = (\epsilon_C/\epsilon_M)([C]_i/[M]_i) \quad (2)$$

where ϵ denotes molar absorptivities, and x_i represents absorption fractional contributions. Because the complex formation constant $K = [C]/[M][Q]$, eq 2 becomes,

$$(x_{C,i}/x_{M,i})(A_C^0/A_M^0) = K[Q]_i(\epsilon_C/\epsilon_M) \quad (3)$$

where Q represents the quencher. After a rearrangement,

$$(x_{C,i}/x_{M,i})/[Q]_i = K(A_C^0/A_M^0)(\epsilon_C/\epsilon_M) \quad (4)$$

Both sides of eq 4 (through x and A^0) are functions of the limit for the pure complex absorption spectrum. However, because the right side of eq 4 becomes a constant as soon as a limit is chosen, the equation requires the selection of a correct limit so that $(x_{C,i}/x_{M,i})/[Q]_i$ is constant with respect to all observed absorption spectra ($i = 1, n$) at different quencher concentrations. This requirement serves as an independent constraint for a determination of the pure complex absorption spectrum. The spectrum of the C_{60}–DMA complex thus obtained is shown in Figure 2.

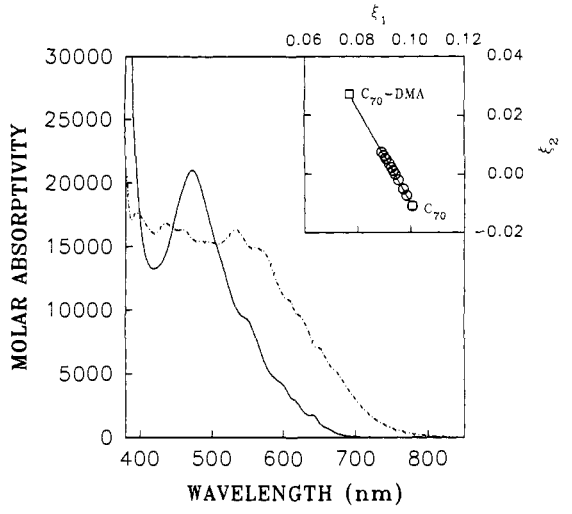

Figure 3. The absorption spectra of the C_{70} monomer (—) and the C_{70}–DMA complex (– • –) from the spectral resolution method. The insert is a plot of combination coefficients.

The absorption spectrum of the C_{70}–DMA complex was determined in a similar fashion. As shown in Figure 3, the complex absorption spectrum is very broad compared to the spectrum of the C_{70} monomer.

The formation constant K was independently determined from the Benesi–Hildebrand plot.[19] For the C_{60}–DMA complex, $K = 0.07 \pm 0.01$ M^{-1}.[9a,10] The uncertainty reflects variations in K for the plots at different wavelengths. With a known K value, molar absorptivities of the complex can be calculated from eq 4. For the C_{60}–DMA complex, the molar absorptivity at the band maximum (536 nm) is 11 800 M^{-1} cm^{-1}, significantly larger than that of the C_{60} monomer. For the C_{70}–DMA complex, $K = 0.09 \pm 0.01$ M^{-1} and the molar absorptivity at the 534-nm peak is 16 300 M^{-1} cm^{-1}.

Fluorescence Quenching in Hexane. For C_{60} and C_{70} in room temperature hexane at low DEA and DMA concentrations (≤0.25 M), contributions of ground state complexes are not significant. The absorption spectrum of C_{70} is essentially the same with respect to changes in DEA and DMA concentration. For C_{60}, only a slight increase of absorbance with increasing DEA and DMA concentration was observed. However, the fluorescence spectra of both C_{60} and C_{70} change dramatically with varying DEA and DMA concentration. The spectral changes are attributed to emission contributions from C_{60}/C_{70}–DEA/DMA exciplexes.

C_{70}–DEA. Fluorescence spectra of C_{70} in hexane at DEA concentrations varying from 0 to 0.176 M are shown in Figure 4. The spectrum in neat hexane shows well-resolved fine structure.[4] As the DEA concentration increases, a decrease of intensities at the shorter wavelength side of the structured band is accompanied by a growing of a broad band at the longer wavelength side of the spectrum. The broad band is assigned to the C_{70}–DEA exciplex.[9b] The decrease of intensities at the structured C_{70} monomer band is also a result of the exciplex formation because excited monomer molecules are quenched in the process (Figure 4). Quantitative characterization of the exciplex formation was accomplished by use of principal component analysis–self modeling spectral resolution.

The data matrix for the analysis consists of 200 fluorescence spectra obtained at 8 different DEA concentrations from 0 to

(19) Benesi, H.; Hildebrand, J. H. *J. Am. Chem. Soc.* **1949**, *71*, 2703.

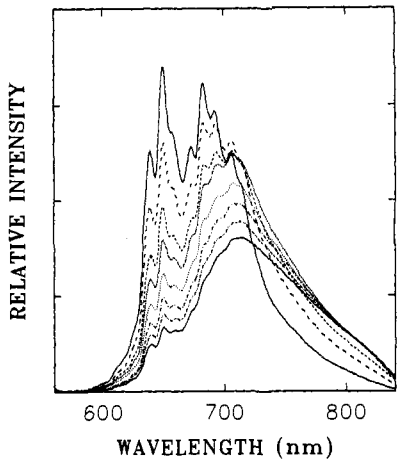

Figure 4. Observed fluorescence spectra of C_{70} (6×10^{-6} M) in room temperature hexane at different DEA concentrations. The DEA concentrations are (in the order of decreasing intensity at the 650-nm peak of the spectra) 0, 0.025, 0.050, 0.075, 0.101, 0.126, 0.151, and 0.176 M.

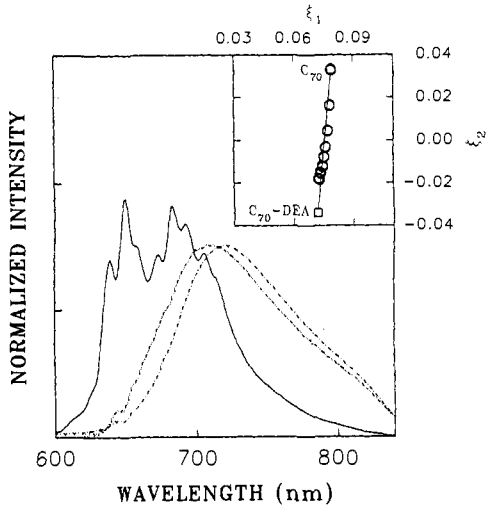

Figure 5. The fluorescence spectra of the C_{70} monomer (—), the C_{70}–DEA exciplex (– · –), and the C_{70}–DMA exciplex (– · · –) from the spectral resolution method. The insert is a plot of combination coefficients for the C_{70}–DEA system.

0.176 M (25 repeat measurements for each concentration). The eigenvalues indicate that the data matrix can be treated as a two-component system. The combination coefficients ξ_{i1} and ξ_{i2} adhere to the normalization line closely, also consistent with a two-component system. The two underlying components in the spectral mixtures are the fluorescence spectra of the C_{70} monomer and the C_{70}–DEA exciplex. The monomer spectrum is known and the exciplex band can be determined by spectral resolution. Because the exciplex band is at the longer wavelength side of the monomer spectrum, it is reasonable to assume that there is a wavelength region at the blue onset of the monomer spectrum where the exciplex emission has no contribution. Therefore, the Lawton–Sylvestre boundary condition[12] can be applied. The limit thus obtained yields the broad exciplex fluorescence spectrum shown in Figure 5.

With the determination of the exciplex limit, relative contributions of the monomer and exciplex emissions were calculated. However, in order to convert the calculated relative emission contributions to relative fluorescence quantum yields, the monomer and exciplex fluorescence spectra obtained from the spectral resolution method (Figure 5) have to be corrected for nonlinear instrumental response. This is not an easy task for the long wavelength region (>800 nm) where the sensitivity of the instrument is stretched to the limit and an accurate determination of the correction factors is almost impossible. We thus introduced

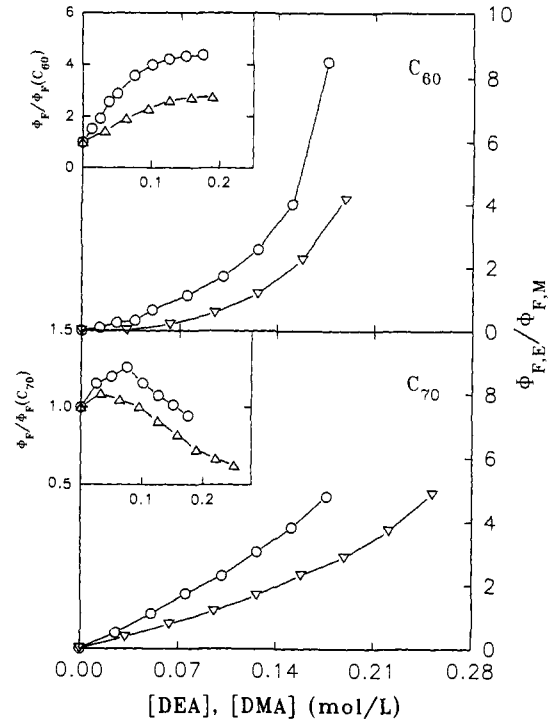

Figure 6. The ratio of fluorescence quantum yields of exciplex and monomer as a function of DEA (○) or DMA (▽) concentrations. The inserts are the total fluorescence quantum yields at different DEA (○) or DMA (△) concentrations.

an assumption that the corrected exciplex band can be approximated by a Gaussian (on the wavenumber scale). The assumption is based on the fact that most exciplex bands have a Gaussian shape due to a distribution of transitions from the excited state complex to the repulsive part of the ground state potential energy curve.[20] As a result, the integrated spectral area under the corrected exciplex band can be estimated by using the portion of the spectrum in the wavelength region <800 nm. Shown in Figure 6 is a plot of the estimated relative fluorescence quantum yields for the C_{70} monomer and the C_{70}–DEA exciplex as a function of DEA concentration.

Total fluorescence quantum yields of the spectral mixtures were estimated in a similar fashion on the basis of the assumption of a Gaussian exciplex band. Ā plot of the total fluorescence yields at different DEA concentrations is shown in Figure 6. The total yield first increases and then decreases with increasing DEA concentration.

C_{70}–DMA. In a hexane solution, changes in fluorescence spectra of C_{70} with increasing DMA concentration are similar to those observed for C_{70}–DEA. Principal component analysis–self modeling spectral resolution was also applied to analyze quantitatively the fluorescence spectral mixtures of the C_{70} monomer and exciplex. The pure exciplex fluorescence band is shown in Figure 5, and the relative fluorescence quantum yields of the C_{70} monomer and the C_{70}-DMA exciplex are shown in Figure 6. The dependence of the ratio of exciplex and monomer fluorescence quantum yields ($\Phi_{F,E}/\Phi_{F,M}$) on DMA concentration for the C_{70}–DMA exciplex is similar to the dependence on DEA concentration for the C_{70}–DEA exciplex. In addition, changes in the total fluorescence quantum yields with increasing DMA concentration follow the same pattern as that for the C_{70}–DEA exciplex, except that the turning point from increasing to decreasing yield is at a lower quencher concentration for C_{70}–DMA (Figure 6).

C_{60}–DEA. Similar to C_{70}, fluorescence spectra of C_{60} also change with increasing DEA concentration (0–0.18 M) in a hexane solution. Although the changes do not appear as dramatic as

(20) Turro, N. J. *Modern Molecular Photochemistry*; Benjamin: Menlo Park, CA, 1978.

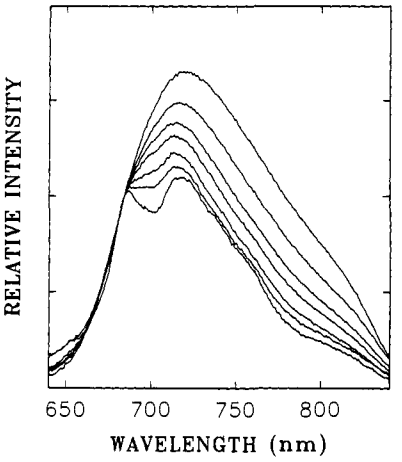

Figure 7. Observed fluorescence spectra of C_{60} (5×10^{-5} M) in room-temperature hexane at different DEA concentrations. The DEA concentrations for the spectra (in the order of increasing intensity at 720 nm) are 0, 0.013, 0.025, 0.050, 0.075, 0.126, and 0.176 M.

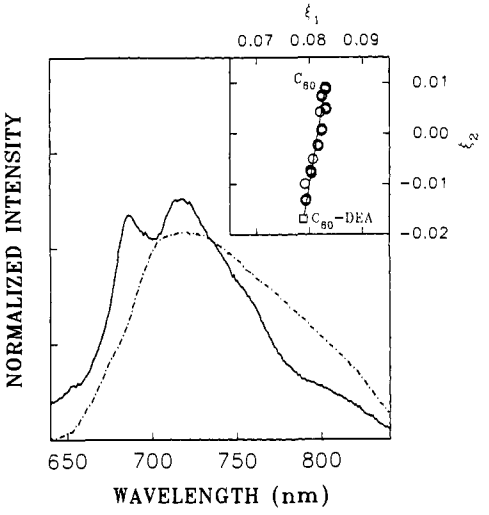

Figure 8. The fluorescence spectra of the C_{60} monomer (—) and the C_{60}–DEA exciplex (– · –) from the spectral resolution method. The insert is a plot of combination coefficients.

those observed for C_{70} because the fluorescence spectrum of the C_{60} monomer has little fine structure, the increasing intensities at the longer wavelength side of the spectra indicate the growing of a new emission band (Figure 7). Similarly, the systematic fluorescence spectral changes can be attributed to C_{60}–DEA exciplex formation. Principal component analysis of the data matrix consisting of 200 fluorescence spectra of C_{60} at different DEA concentrations indicated that the observed fluorescence spectra are also two-component mixtures. The pure exciplex fluorescence spectrum was determined from the Lawton–Sylvestre boundary condition by assuming that the exciplex band is somewhat shifted to longer wavelengths from the C_{60} monomer spectrum. As shown in Figure 8, the spectrum of the C_{60}–DEA exciplex is a broad and structureless band, similar to those of C_{70} exciplexes presented above. The ratio of fluorescence quantum yields of the C_{60}–DEA exciplex and the C_{60} monomer is also plotted as a function of DEA concentration in Figure 6. Similar to the results for C_{70} exciplexes, the dependence of the ratio $\Phi_{F,E}/\Phi_{F,M}$ on DEA concentration shows an upward curvature. As shown in Figure 6, the total fluorescence quantum yields first increase with increasing DEA concentration and then level off at higher DEA concentrations.

C_{60}–DMA. C_{60} also forms an exciplex with DMA in a room temperature hexane solution. As shown in Figure 6, the results for the C_{60}–DMA exciplex from the spectral resolution method are similar to those for the C_{60}–DEA exciplex.

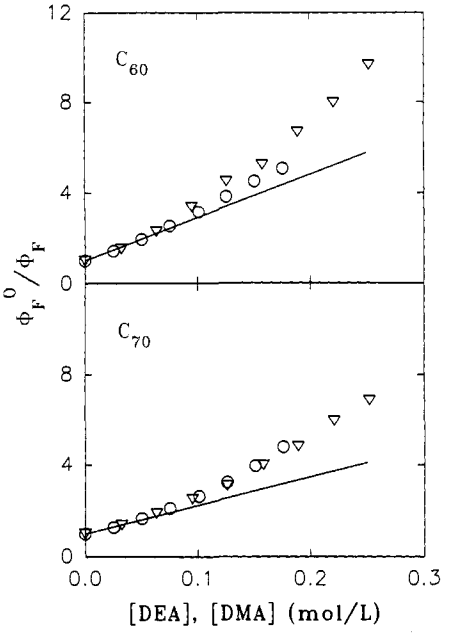

Figure 9. The fluorescence quenching ratio Φ_F^0/Φ_F for C_{60} and C_{70} in room temperature toluene at different DEA (○) and DMA (▽) concentrations.

Fluorescence Quenching in Toluene. For C_{60} and C_{70} in a room temperature toluene solution with low concentrations of DEA and DMA (≤0.25 M), contributions from ground state complexes are also not significant. The absorption spectra are almost the same as those in hexane. However, no exciplex fluorescence is observed.

C_{70}–DMA/DEA. In a toluene solution, the fluorescence intensities of C_{70} are quenched effectively by DEA and DMA, but the spectral shape hardly changes at all. The observed fluorescence spectra consist of no contributions from any exciplex emissions.

Ratios of fluorescence quantum yields without (Φ_F^0) and with (Φ_F) quencher are plotted as a function of quencher concentration in Figure 9. The results for DEA and DMA are almost the same. According to the Stern–Volmer equation, a linear relationship between the quenching ratio Φ_F^0/Φ_F and quencher concentration is expected,

$$\Phi_F^0/\Phi_F = 1 + K_{SV}[Q] \quad (5)$$

where K_{SV} is the Stern–Volmer constant. For the results in Figure 9, upward deviations from the Stern–Volmer relationship (eq 5) are obvious, especially at high quencher concentrations. An estimate of the Stern–Volmer constant can be made by considering only the data points at low quencher concentrations. Because the quenching by DEA and DMA is virtually the same, the two sets can be treated together. For the data points at [Q] < 0.1 M, a K_{SV} value of 16 M^{-1} was obtained from a least-squares fit (Figure 9).

C_{60}–DEA/DMA. There are also no emissions from C_{60}–DEA and C_{60}–DMA exciplexes in a toluene solution. As the DEA and DMA concentration increases, the fluorescence intensities are quenched without change in spectral shape. Shown in Figure 9 are plots of the quenching ratio Φ_F^0/Φ_F as a function of quencher concentration, which similarly show upward deviations from the Stern–Volmer relationship. The quenching by DEA and DMA is also very similar, and therefore a single plot is used. If only the data points at [Q] < 0.1 M are considered, a Stern–Volmer constant K_{SV} of 23 M^{-1} is obtained (Figure 9).

Discussion

The results presented above indicate that C_{60} and C_{70} form both ground and excited state complexes with DEA and DMA.

These are charge transfer complexes, with DEA and DMA as electron donors and C_{60} and C_{70} as electron acceptors. The complexes with DEA and DMA have similar spectroscopic properties.

An important feature in the absorption spectra of C_{60} ground state complexes is the significant increase in molar absorptivity. From the C_{60} monomer to the C_{60}–DMA complex, the integrated molar absorptivity (430–750 nm) is increased from 4.6×10^6 to 7.5×10^7. The dramatic increase of transition probabilities can be explained by a reduction of C_{60} symmetry upon complexation.[9a] It also explains the result that from C_{70} to C_{70}-DMA complexes the integrated molar absorptivity is virtually unchanged. The formation equilibrium constants for the ground state complexes are small, so that the possibility of contact (or collision) charge transfer complexes[21-23] should be considered. To the extreme, it could be argued that the absorption spectral changes due to the presence of DMA are a result of solvent perturbation, rather than the formation of complexes. Our results seem to support the complexation mechanism because it will be an unusual coincidence for the solvent perturbation to show up as a nearly perfect second component in principal component analysis. However, as an interesting issue, it should be examined further with other experimental techniques.

The emissions of C_{60} and C_{70} monomers are quenched effectively by DEA and DMA. At low DEA and DMA concentrations ($\leq$0.25 M) in a room temperature hexane solution, the quenching of C_{60} and C_{70} excited states is dominated by the formation of C_{60}/C_{70}–DEA/DMA exciplexes. However, as the solvent is changed from hexane to toluene, the behavior of C_{60}/C_{70}–DEA/DMA systems becomes very different. In a room temperature toluene solution, no emissions from C_{60}/C_{70}–DEA/DMA exciplexes can be observed.

It is generally understood that exciplex formation is affected by solvent properties such as viscosity and polarity.[24] Solvent viscosity primarily affects the diffusion process in the quenching of excited monomer molecules. For the change of behavior from hexane to toluene, the viscosity effect should not be a dominating factor because the viscosities of the two solvents are similar (0.326 and 0.590 cP for hexane and toluene at 20 °C, respectively) and fluorescence intensities of C_{60} and C_{70} are effectively quenched in toluene. It is more likely that the lack of exciplex emission in toluene is a result of higher solvent polarizability. In toluene, there could also be C_{60} and C_{70} excited state complexes with DEA and DMA. The complexes are non-emissive probably because of efficient competing processes such as the formation of solvated ions.[25] A recent ESR study has shown that the C_{60} radical anion can be detected on photolysis of C_{60} in the presence of electron donors such as DEA.[26] Because toluene is a more polarizable solvent than hexane (refractive index 1.496 for toluene vs 1.375 for hexane), it can make the charge separation process more efficient. Such an explanation based on solvent polarizability effect is also consistent with the spectroscopic results already in the literature. While C_{70}–DEA exciplex fluorescence was observed in a methylcyclohexane solution,[9b] there was no exciplex emission for C_{70}–DMA in room temperature benzene.[10,27] Nevertheless, the extreme solvent sensitivity of C_{60}/C_{70}–DMA/DEA exciplexes is somewhat unusual.[25]

As shown in Figure 9, the quenching results in toluene at low DEA and DMA concentrations can approximately be described by the Stern–Volmer equation. The Stern–Volmer constant K_{SV} is expressed as,

$$K_{SV} = k_q \tau_f \tag{6}$$

where τ_f is the fluorescence lifetime of the molecule being quenched and k_q is the quenching rate constant. For the fluorescence lifetimes of C_{60} and C_{70}, quite different experimental values have been reported.[27-30] Because C_{70} is more fluorescent, a measurement of fluorescence decay should be more favorable experimentally. Thus, τ_f of 660 ps from the time-correlated single photon counting method[29] is considered a reliable value for C_{70}. It is also in excellent agreement with the result of 670 ps from a recent transient absorption study.[30] From the Stern–Volmer constant obtained by considering only the data points at low quencher concentrations, a k_q of 2.4×10^{10} M^{-1} s^{-1} is calculated from eq 6. If the same quenching rate constant is assumed for C_{60}, the ratio of Stern–Volmer constants for C_{60} and C_{70} is the ratio of their fluorescence lifetimes. With a Stern–Volmer constant of 23 M^{-1} for C_{60} obtained under the same conditions as those for C_{70}, the ratio of C_{60} and C_{70} fluorescence lifetimes is predicted to be 1.44. This puts the C_{60} fluorescence lifetime at $\sim$1 ns. A more accurate determination of the fluorescence lifetime ratio can be achieved by taking into account the curvature in the Stern–Volmer plots.

As shown in Figure 9, plots of the fluorescence quenching ratio Φ_F^0/Φ_F vs [DEA] and [DMA] for C_{60} and C_{70} show upward deviations from the Stern–Volmer relationship. The deviations are attributed to static fluorescence quenching. The results can be treated by the following equation:[31]

$$\Phi_F^0/\Phi_F = (1 + K_{SV}[Q]) \exp(Nv[Q]) \tag{7}$$

where N is Avogadro's number and v is the static quenching volume. By treating the results of DEA and DMA in a single plot, least-squares fits based on eq 7 yield K_{SV} and v respectively of 13 M^{-1} and 5300 Å^3 for C_{60}, and 8.1 M^{-1} and 5800 Å^3 for C_{70} (Figure 10). The ratio of the Stern–Volmer constants for C_{60} and C_{70} is 1.6. The result supports a recent assessment[3] that the fluorescence lifetime of C_{60} in room temperature solutions should be around 1.2 ns. The diffusion-controlled quenching rate constant of 1.2×10^{10} M^{-1} s^{-1} from eq 7 is more reasonable than the value of 2.4×10^{10} M^{-1} s^{-1} from the plots in Figure 9.[32] If a spherical static quenching volume is assumed, the v values correspond to static fluorescence quenching radii of 10.8 and 11.1 Å for C_{60} and C_{70}, respectively, comparable to the sum of molecular radii of the fullerene–quencher pairs.

Similar upward deviations from the Stern–Volmer relationship have been observed for the quenching of C_{70} fluorescence by strong electron donors such as *N,N*-dimethyl-*p*-toluidine.[27] A static quenching mechanism that assumes ground state 1:1 complexation between C_{70} and quencher molecules was proposed,[27]

(21) By definition contact (or collision) complexes have zero equilibrium constant and infinite molar absorptivity from the Benesi–Hildebrand plot.[22] However, intermediate situation with substantial contributions from contact (or collision complexes) is also a possibility.[23]

(22) (a) Orgel, L. E.; Mulliken, R. S. *J. Am. Chem. Soc.* **1957**, *79*, 4839. (b) Murrell, J. N. *Q. Rev. (London)* **1961**, *15*, 191. (c) Mulliken, R. S.; Person, W. B. *Molecular Complexes*; Wiley-Interscience: New York, 1969, p 390.

(23) (a) Hanna, M. W.; Lippert, J. In *Molecular Complexes*; Foster, R., Ed.; Crane, Russak & Company: New York, 1974; Vol. 1, p 14. (b) Foster, R. In *Molecular Complexes*; Foster, R., Ed., Crane, Russak & Company: New York, 1974; Vol. 2, p 110.

(24) Bhattacharyya, K.; Chowdhury, M. *Chem. Rev.* **1993**, *93*, 507.

(25) Birks, J. B. In *Organic Molecular Photophysics*; Birks, J. B., Ed.; Wiley: London, 1975; Vol. 2, p 529 and references cited therein.

(26) Krusic, P. J.; Wassenman, E.; Parkinson, B. A.; Malone, B.; Holler, E. R., Jr. *J. Am. Chem. Soc.* **1991**, *113*, 6274.

(27) Williams, R. M.; Verhoeven, J. W. *Chem. Phys. Lett.* **1992**, *194*, 446.

(28) (a) Sension, R. J.; Phillips, C. M.; Szarka, A. Z.; Romanow, W. J.; McGhie, A. R.; McCauley, J. P., Jr.; Smith, A. B.; Hochstrasser, R. M. *J. Phys. Chem.* **1991**, *69*, 6075. (b) Wasielewski, M. R.; O'Neil, M. P.; Lykke, K. R.; Pellin, M. J.; Gruen, D. M. *J. Am. Chem. Soc.* **1991**, *113*, 2774.

(29) Kim, D.; Lee, M.; Suh, Y. D.; Kim, S. K. *J. Am. Chem. Soc.* **1992**, *114*, 4429.

(30) (a) Tanigaki, K.; Ebbesen, T. W.; Kuroshima, S. *Chem. Phys. Lett.* **1991**, *185*, 189. (b) Ebbesen, T. W.; Tanigaki, K.; Kuroshima, S. *Chem. Phys. Lett.* **1991**, *181*, 501.

(31) Birks, J. B. *Photophysics of Aromatic Molecules*; Wiley-Interscience: London, 1970.

(32) Saltiel, J.; Atwater, B. W. *Adv. Photochem.* **1988**, *14*, 1.

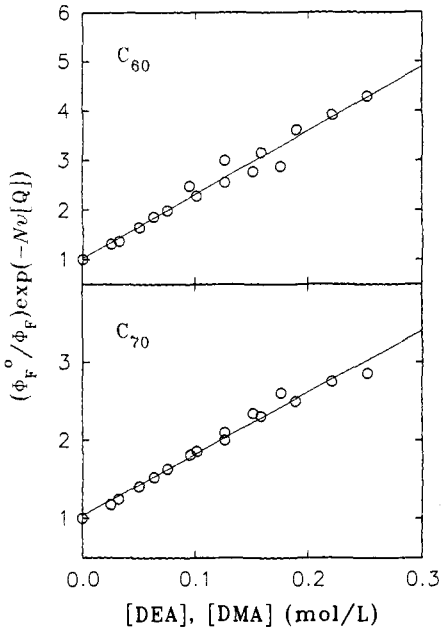

Figure 10. A treatment for the results of fluorescence quenching of C_{60} and C_{70} by DEA and DMA in room temperature toluene based on a model in which both static and dynamic quenchings are considered.

$$\Phi_F^0/\Phi_F = (1 + K_S[Q])(1 + K_{SV}[Q]) \quad (8)$$

where K_S is the formation constant of the ground state 1:1 complex. The equation can be reorganized as follows;

$$(\Phi_F^0/\Phi_F - 1)/[Q] = (K_S + K_{SV}) + K_S K_{SV}[Q] \quad (9)$$

With an application of the mechanism to the quenching of C_{70} fluorescence by DEA, a plot of $(\Phi_F^0/\Phi_F - 1)/[Q]$ vs [Q] is linear (slope = 65, intercept = 10, and correlation coefficient = 0.997). However, K_S and K_{SV} cannot be calculated from the slope and intercept values because no real solutions can be found. If the equilibrium constant obtained from the Benesi–Hildebrand plot is used as K_S, a plot of $(\Phi_F^0/\Phi_F)/(1 + K_S[Q])$ vs [Q] is almost equally nonlinear as the Stern–Volmer plot. Similar results were obtained for the other systems (C_{70}–DMA, C_{60}–DEA, and C_{60}–DMA). Therefore, the mechanism represented by eq 8 is not applicable to the quenching results presented here.

For the formation of exciplexes in a hexane solution, the mechanism suggested by Hui and Ware for the anthracene–DMA system was considered.[33] Because the observed monomer fluorescence yield $\Phi_{F,M}$ consists of contributions from both the prompt $\Phi_{F,MP}$ and delayed $\Phi_{F,MD}$ monomer emissions, the fluorescence quantum yield ratio of the equilibrating excited monomer (M*) and exciplex (E*) is the following:

$$\Phi_{F,E}/(\Phi_{F,M} - \Phi_{F,MP}) = k_{F,E}[E^*]/k_{F,M}[M^*] = K_1(k_{F,E}/k_{F,M})[Q] \quad (10)$$

where $k_{F,M}$ and $k_{F,E}$ are fluorescence radiative rate constants of the monomer and exciplex, respectively, and K_1 is the equilibrium constant for $M^* + Q \rightleftarrows E^*$. If the prompt fluorescence yield $\Phi_{F,MP}$ is assumed to be negligible, eq 10 predicts a linear relationship (through the origin) between the observed fluorescence quantum yield ratio $\Phi_{F,E}/\Phi_{F,M}$ and quencher concentration [Q]. For C_{60}/C_{70}–DEA/DMA exciplexes, plots of the ratio $\Phi_{F,E}/\Phi_{F,M}$ vs [Q] are hardly linear (Figure 6), indicating that the excited state mechanism is more complicated.

It is likely that the assumption of negligible $\Phi_{F,MP}$ is invalid and that the upward curvatures in the dependence of the observed fluorescence quantum yield ratio $\Phi_{F,E}/\Phi_{F,M}$ on [Q] for C_{70} are actually due to contributions of the prompt monomer emission. As discussed above for C_{70} in toluene, the fluorescence is effectively quenched by DEA and DMA through both dynamic and static processes. However, even at a DMA concentration of 0.25 M, the quenching is still not complete. The residual prompt emission can be significant if the delayed fluorescence from the equilibrating monomer excited state is very weak. Equation 10 can be rewritten as follows:

$$\frac{\Phi_{F,E}/\Phi_{F,M}}{(1 - \Phi_{F,MP}/\Phi_{F,M})} = K_1(k_{F,E}/k_{F,M})[Q] \quad (11)$$

The term $\Phi_{F,MP}/\Phi_{F,M}$ can be expressed as,

$$\Phi_{F,MP}/\Phi_{F,M} = (\Phi_{F,M}^0/\Phi_{F,M})/(\Phi_{F,M}^0/\Phi_{F,MP}) \quad (12)$$

where $\Phi_{F,M}^0$ is the monomer fluorescence yield in the absence of the quencher. Both $(\Phi_{F,M}^0/\Phi_{F,M})$ and $(\Phi_{F,M}^0/\Phi_{F,MP})$ are quencher concentration dependent. The former can be obtained from the fractional contributions of monomer fluorescence, which are the results from principal component analysis–self modeling spectral resolution of the fluorescence spectral mixtures, and the latter can be written as eq 7. Thus,

$$\frac{(\Phi_{F,E}/\Phi_{F,M})}{[Q]}\left[1 - \frac{(\Phi_{F,M}^0/\Phi_{F,M})}{(1 + K_{SV}[Q])\exp(Nv[Q])}\right]^{-1} = K_1(k_{F,E}/k_{F,M}) \quad (13)$$

Obviously, the right side of the equation is a constant independent of quencher concentration. With a selection of the correct quenching parameters k_q and v, the left side of the equation should be independent of quencher concentration as well. As discussed for C_{70} in a toluene solution, the fluorescence quenching by DEA and DMA is diffusion-controlled (K_{SV} = 8.1 M^{-1} and $k_q = 1.2 \times 10^{10}$ M^{-1} s^{-1}). In hexane, the diffusion-controlled quenching rate constant should be larger because of lower solvent viscosity. According to the Debye equation,[32]

$$k_q(\text{hexane})/k_q(\text{toluene}) = \eta(\text{toluene})/\eta(\text{hexane}) \quad (14)$$

where η denotes solvent viscosity. The k_q in a hexane solution thus obtained is 2.2×10^{10} M^{-1} s^{-1}. The static fluorescence quenching volume v for C_{70} in hexane is determined as a parameter in such a way that the variation in the left side of eq 13 is forced to a minimum. A v value of 8100 Å^3 optimized for both C_{70}–DEA and C_{70}–DMA is obtained. It is interesting that the static quenching radius of C_{70} in hexane (12.4 Å) is somewhat larger than that in toluene. As shown in Figure 11, even with contributions of the delayed monomer emission (which accounts for $\sim^1/_3$ of the observed monomer fluorescence yield at [DEA] = 0.17 M) the decrease of monomer fluorescence yield with increasing quencher concentration is faster in hexane than in toluene.

The constant $K_1(k_{F,E}/k_{F,M})$, eq 13, is 91.5 for C_{70}–DEA and 35.5 for C_{70}–DMA. If the radiative rate constant $k_{F,E}$ is assumed to be the same for C_{70}–DEA and C_{70}–DMA, the equilibrium constant K_1 for the C_{70}–DEA exciplex is 2.6-times larger than that for the C_{70}–DMA exciplex. Thus, the energy of the C_{70}–DEA exciplex is 0.55 kcal/mol (195 cm^{-1}) lower than that of C_{70}–DMA, with the assumption that there is no difference in their entropies. This is in surprisingly good agreement with the observed fluorescence spectral shift. As shown in Figure 5, the emission band maximum of the C_{70}–DEA exciplex is $\sim$10 nm (or 196 cm^{-1}) red-shifted from that of the C_{70}–DMA exciplex.

A reasonable estimate of the ratio $k_{F,E}/k_{F,M}$ is necessary for a determination of the equilibrium constant K_1. By calculating the transition probabilities of the C_{70} exciplex emission from the

(33) Hui, M.-H.; Ware, W. R. *J. Am. Chem. Soc.* **1976**, *98*, 4718.

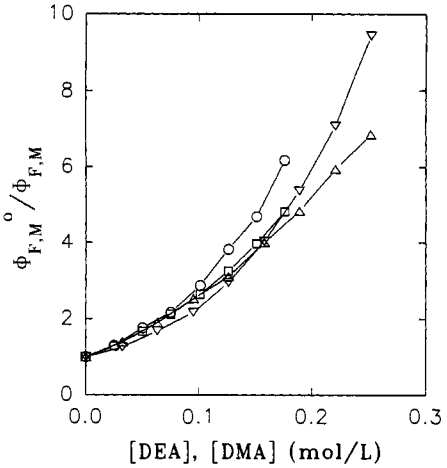

Figure 11. The quenching ratio for the C_{70} monomer fluorescence in hexane [DEA (○) and DMA (▽)] and toluene [DEA (□) and DMA (△)]. The $\Phi_{F,M}$ values in hexane are obtained from the results of principal component analysis–self modeling spectral resolution of the fluorescence spectral mixtures.

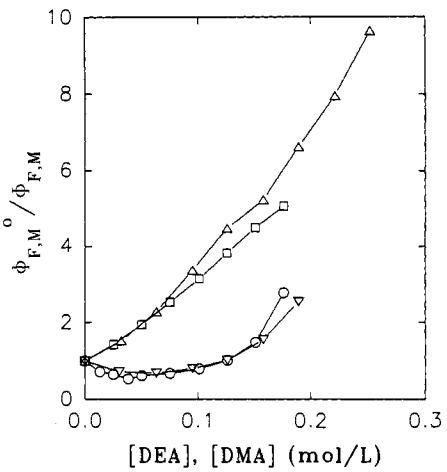

Figure 12. The quenching ratio for the C_{60} monomer fluorescence in hexane [DEA (○) and DMA (▽)] and toluene [DEA (□) and DMA (△)]. The $\Phi_{F,M}$ values in hexane are obtained from the results of principal component analysis–self modeling spectral resolution of the fluorescence spectral mixtures.

molar absorptivities of C_{70} ground state charge transfer complexes, a $k_{F,E}$ of 8×10^7 s^{-1} is obtained on the basis of the Strickler–Berg equation.[34] For the C_{70} monomer, it has been shown[4] that the $k_{F,M}$ determined experimentally from the fluorescence quantum yield and lifetime differs by two orders of magnitude from the calculated value. In order to be consistent with the calculation of $k_{F,E}$, a $k_{F,M}$ value of 9×10^7 s^{-1} calculated on the basis of the first absorption band of the C_{70} monomer is used. Thus, the equilibrium constant K_1 for C_{70}–DEA is ~100, which corresponds to a free energy difference of 2.7 kcal/mol between the C_{70}–DEA exciplex and the excited C_{70} monomer at room temperature.

Although the treatment discussed above shows that the results can be accounted for by using the mechanism of Hui and Ware,[33] it does not necessarily rule out other possibilities. For example, there is a possibility that the upward curvature in the plots of $\Phi_{F,E}/\Phi_{F,M}$ vs [Q] at high concentrations is partially due to the quenching of exciplexes and/or the formation of C_{70}–quencher 1:2 exciplexes. For systems such as anthracene–DMA, substantial contributions of exciplex–DMA interactions in the excited state processes were observed.[24,35,36] However, because the results from principal component analysis have shown that there is only one exciplex component in the fluorescence spectral mixtures, the spectra of 1:1 and 1:2 exciplexes must be identical or contributions of the 1:2 exciplex are very small. Considering the quencher concentrations used here are relatively low and the exciplex lifetime is relatively short (on the order of 400 ps),[10] we believe that the participation of 1:2 exciplexes is limited. Although in principle the excited state parameters discussed above will be somewhat different if there are indeed contributions due to exciplex–quencher interactions, our data are insufficient for a rigorous treatment that considers prompt fluorescence, static quenching, and exciplex–quencher interactions simultaneously.

The situation is more complicated for C_{60}–DEA/DMA, to which eq 13 is not applicable. As shown in Figure 12, the observed monomer fluorescence quantum yield changes with quencher concentration in an unusual pattern. At low quencher concentrations, the observed yields are actually larger than those in the absence of quenchers. Such an increase of monomer fluorescence yield with increasing quencher concentration cannot be explained in the context of the mechanism by Hui and Ware.[33] Typically, if the prompt and delayed emissions are from somewhat different excited states, an increase of fluorescence yield with increasing quencher concentration is possible if the delayed emission has a higher yield. However, the question is why similar results are not observed in a toluene solution. For C_{60}–DEA/DMA, direct excitation of ground state charge transfer complexes is also a possibility. As discussed earlier, there are slight changes in absorption spectra of C_{60} even at low DEA and DMA concentrations (≤0.25 M). With some excited complexes generated by a direct excitation,[35] it is possible (at least in principle) that the monomer fluorescence yields in the presence of quenchers can be larger than those in the absence of quenchers. Further investigations are required in order to address this issue more clearly.

In summary, C_{60} and C_{70} form ground state charge transfer complexes and exciplexes with DEA or DMA at high and low DEA/DMA concentrations, respectively. The pure absorption spectra of ground state complexes and exciplex fluorescence spectra of C_{60}/C_{70}–DEA/DMA are determined by use of a chemometrics method principal component analysis–self modeling spectral resolution. The exciplex emissions are strongly solvent dependent. The quenching of C_{60}/C_{70} monomer fluorescence involves both dynamic and static processes. The observed dual fluorescence for C_{60}/C_{70}–DEA/DMA in hexane can be explained by a mechanism in which contributions from both prompt and delayed monomer emissions are considered.

Acknowledgment. Financial support from the donors of the Petroleum Research Fund, administered by the American Chemical Society, from the National Science Foundation (CHE-9320558), and from a Clemson University Research Grant is gratefully acknowledged.

(34) Strickler, S. J.; Berg, R. A. *J. Chem. Phys.* **1962**, *37*, 814.

(35) For example, see: (a) Yang, N. C.; Shold, D. M.; Kim, B. *J. Am. Chem. Soc.* **1976**, *98*, 6587. (b) Saltiel, J.; Townsend, D. E.; Watson, B. D.; Shannon, P.; Finson, S. L. *J. Am. Chem. Soc.* **1977**, *99*, 884.

(36) (a) Pearson, J. M.; Turner, S. R. In *Molecular Association*; Forster, R., Ed.; Academic Press: London, 1979; Vol. 2, p 79. (b) Davidson, R. S. In *Advances in Physical Organic Chemistry*; Gold, V., Bethell, D., Eds.; Academic Press: New York, 1983; Vol. 19, p 1.